Engineering Notes

ENGINEERING NOTES are short manuscripts describing new developments or important results of a preliminary nature. These Notes cannot exceed 6 manuscript pages and 3 figures; a page of text may be substituted for a figure and vice versa. After informal review by the editors, they may be published within a few months of the date of receipt. Style requirements are the same as for regular contributions (see inside back cover).

Roughness Effects on Heat Transfer from a NACA 0012 Airfoil

Philip E. Poinsatte* and G. James Van Fossen*
NASA Lewis Research Center, Cleveland, Ohio 44135
and
Kenneth J. De Witt†
University of Toledo, Toledo, Ohio 43606

Introduction

A THERMAL analysis of the aircraft ice accretion phenomenon shows that convective and evaporative cooling are the dominant loss terms in the energy balance.[1] Since both the convective and evaporating cooling are proportional to the local convective heat transfer coefficient h, a good characterization of the convective heat transfer is necessary to accurately model the icing process. One concern is how the behavior of h changes as ice accretes on a surface. As ice grows on a surface, that surface becomes rough, altering the boundary-layer air flow and thus the heat transfer. Recent heat transfer experiments performed by Van Fossen et al.[2] on a cylinder in crossflow under different turbulence and roughness conditions did show that roughness, like that resulting from early ice growth, forced a laminar boundary layer into transition.

The NACA 0012 airfoil cited in Ref. 1 was also used to obtain local convective heat transfer coefficients from a roughened surface. Tests were conducted in the NASA Lewis icing research tunnel (IRT) and on the NASA Lewis Twin Otter aircraft. Surface roughness was added to the airfoil by fastening hemispheres of silver alloy to the surface with cyanoacrylic adhesive. The hemispheres were 2 mm (0.078 in.) in diameter and were attached to the airfoil in different patterns, similar to those employed by Schlichting[3] in his boundary-layer work. These patterns were chosen to facilitate numerical modeling of the roughness in various computer codes.

Three patterns were employed in the flight tests while four were used in the tunnel tests. Figure 1 shows planar sketches of the location of the roughness elements relative to the heat flux gauges for each of the patterns: leading-edge roughness, sparse roughness, dense 1 roughness, and dense 2 roughness. The thermal resistance of the gauge surface was not altered significantly because of the sparse spacing of the elements and the high conductivity of the silver alloy. A numerical heat conduction computer model predicted that the tempertature at the tip of each roughness element was less than 0.28°C (0.5°F) lower than the temperature of the smooth aluminum gauge surface. Also, each roughness element generally increased the heat transfer surface area by only 1% per gauge. No attempt was made to account for the presence of the roughness elements in the data reduction.

The airfoil, test facilities and procedure, and the data reduction method were identical to those used for the smooth airfoil.[1] A complete description is given in Ref. 4.

Results and Discussion

Selected results of the rough surface heat transfer tests conducted in the IRT as well as data obtained in flight are presented here. The data are plotted as Frossling number based on chord ($Fr = Nu/Re^{0.5}$) as a function of dimensionless surface distance s/c (surface distance/chord). Special emphasis is given to the effect on heat transfer of the different freestream turbulence levels. The turbulence intensity measured with hotwire equipment during the flight runs was found to be very low (<0.1%). However, in the IRT with the cloud-making sprays off, the turbulence intensity level was found to be 0.6, 0.52, and 0.7% at tunnel air speeds of 31, 63, and 94 m/s (70, 140, and 210 mph), respectively.

The addition of surface roughness to the leading edge of the airfoil (see Fig. 1a) had little effect on the heat transfer as compared with the smooth cases.[1] It locally increased the stagnation point heat transfer about 10% but did not appear to affect the downstream heat transfer. This increase can be partially explained by the 4% increase in surface area caused by the presence of the hemispherical roughness elements. It could also be attributed to a disturbance of the boundary layer by the relatively huge roughness elements followed by a return to laminar flow sufficiently past the leading-edge trip point.

The flight and tunnel data for the sparsely roughened airfoil (see Fig. 1b) at a 0-deg angle of attack and nominal Reynolds numbers of 1.2×10^6 and 2.4×10^6 are presented in Fig. 2. The axial positions of the roughness elements are denoted by the arrows above the abscissa. The solid line on the figure represents the averaged, smooth-surface, 0-deg angle-of-attack flight data from Ref. 1, and will be reproduced on subsequent figures for reference. Compared with the smooth airfoil case, the sparsely roughened airfoil data show an increase in heat transfer on the stagnation gauge due to a boundary-layer disturbance similar to that of the leading-edge roughness case. Downstream of the stagnation region, the Frossling number exhibits a pattern of increasing at and immediately downstream of the roughness row position, then falling off slightly. Note that the downstream gauges show somewhat higher Frossling numbers for the higher Reynolds number vs the lower Reynolds number case. Power law curve fits of $Nu = A(Re)^B$ showed that at an $s/c > 0.02$ the Nusselt number begins moving to a Reynolds number dependence higher than $Re^{0.5}$. This trend was especially true for the tunnel data and it is an indication of boundary-layer transition.

With few exceptions, the flight and tunnel Frossling number values on most gauges agreed with the calculated 5% uncertainty limits for the low Reynolds number case. At the higher Reynolds number, as was also observed with the smooth airfoil case in Ref. 1, the two tunnel conditions agreed quite well, but most gauges for both cases show tunnel Frossling number

Presented in part as Paper 90-0199 at the AIAA 28th Aerospace Sciences Meeting, Reno, NV, Jan. 8–11, 1990; received Sept. 1, 1990; revision received July 10, 1991; accepted for publication Aug. 14, 1991.

*Aerospace Engineer, Heat Transfer Branch, Internal Fluid Mechanics Division. Member AIAA.
†Professor, Department of Chemical Engineering. Member AIAA.

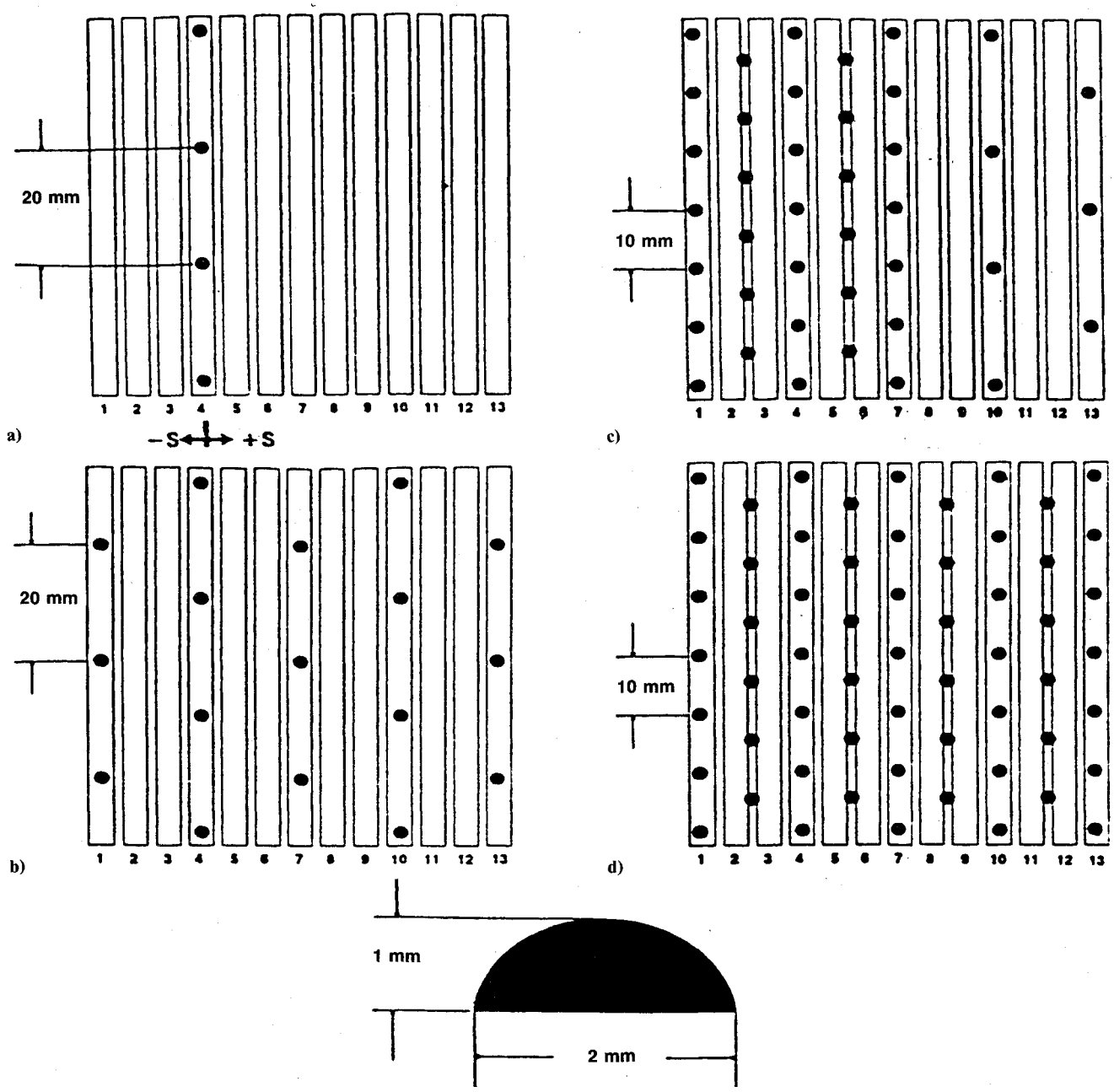

Fig. 1 Roughness element patterns: a) leading-edge roughness, b) sparse roughness, c) dense 1 roughness, and d) dense 2 roughness.

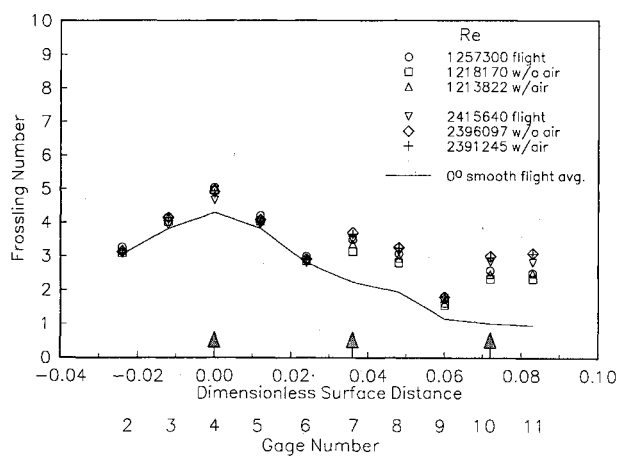

Fig. 2 Frossling number vs dimensionless surface distance: sparse roughness, 0-deg angle of attack, $Re = 1.2 \times 10^6$ and 2.4×10^6, flight and IRT data.

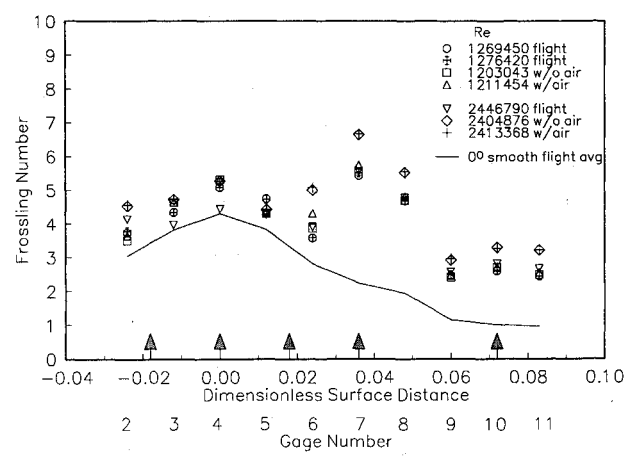

Fig. 3 Frossling number vs dimensionless surface distance: dense 1 roughness, 0-deg angle of attack, $Re = 1.2 \times 10^6$ and 2.4×10^6, flight and IRT data.

values 4–10% higher than corresponding flight values. Similar trends were also observed on the 2- and 4-deg angle-of-attack data, though the 4-deg case exhibited somewhat higher magnitude. Some gauges for the 2.4×10^6 Reynolds number show tunnel heat transfer data up to 16% higher than the flight data.

Increasing the density of the roughness elements from the sparse to the dense 1 pattern (see Fig. 1c) has a dramatic effect on the heat transfer downstream. The data for the 0-deg angle of attack, dense 1 roughened airfoil, are illustrated in Fig. 3. The heat transfer from gauges 2 to 8 is substantially higher than the corresponding sparsely roughened case. Further downstream, past gauge 7, the density of roughness elements decreases, and at gauges 10 and 11, the effect of the increased density of the roughness elements upstream seems to have nearly damped out. This trend indicates that if there is roughness of sufficient magnitude present, the boundary layer is perturbed locally and immediately downstream. However, as the density of roughness is reduced in the downstream direction, the heat transfer recovers to a level that is consistent with the sparse roughness pattern. For the lower Reynolds number of 1.2×10^6, both tunnel data sets again agree; however, they show values 2–8% higher than the flight data. The 2.4×10^6 Reynolds number case illustrates similar behavior, with the tunnel data being 18–25% higher than the flight data. This result is somewhat surprising because it would seem that as the boundary layer is more and more disturbed by the roughness, the freestream turbulence would have less and less effect on the Frossling number. However, in this dense 1 case, the freestream turbulence appears to have a greater effect on the heat transfer than in the sparse roughness cases. Moving to a higher angle of attack did not alter this trend.

Frossling data vs s/c for the 0-deg, dense 2 roughness pattern (see Fig. 1d) are presented for low and high Reynolds number cases in Fig. 4. Note that this graph shows only tunnel data, as no dense 2 flight data were acquired. Examination of Fig. 1 shows that the dense 2 roughness pattern is very similar to the dense 1 roughness pattern, except that the roughness element density is constant throughout and does not decrease at $s/c > 0.04$ as the dense 1 pattern does. As expected, the heat transfer results for the dense 2 pattern are very similar to the results of the dense 1 cases up to s/c of 0.04. For $s/c > 0.04$, the Frossling number in the dense 2 cases, while still falling off from the gauge 7 maximum and then leveling off, is somewhat higher than the dense 1 data. Thus, the dense 2 roughness data exhibit the same heat transfer behavior as the dense 1 cases, except that the dense 2 data yield a higher Frossling number in the region of higher roughness density ($s/c>0.04$). There is no upstream heat transfer effect due to the increase of downstream roughness density.

Generally, it would seem that the IRT is a relatively clean wind tunnel, at least with respect to heat transfer in the forward portion of an airfoil. The slightly higher turbulence level in the tunnel had minimal effect on the heat transfer from the smooth airfoil at the lower Reynolds number; the higher Reynolds number did illustrate a greater turbulence induced heat transfer increase.[1] The addition of surface roughness, however, seemed to magnify somewhat the effect of turbulence on heat transfer. The addition of spray atomizing air had virtually no effect on the smooth or rough surface heat transfer, and it is therefore believed that the spray air did not significantly alter the freestream turbulence level in the tunnel.

The general Frossling number dependence on angle of attack is illustrated in Fig. 5 for the sparsely roughened airfoil. The sparsely roughened airfoil data exhibited behavior similar to the smooth airfoil concerning the aerodynamic stagnation point. As the angle of attack increases, the aerodynamic stagnation point moves from gauge 4 toward gauge 3, which effectively has a larger leading edge radius, thereby resulting in a lower heat transfer coefficient on gauge 3. The flow then accelerates around the leading edge, which increases the heat transfer at the geometric stagnation point (gauge 4). The downstream gauges, meanwhile, show the heat transfer increasing with increasing angle of attack. The other roughness cases exhibited similar angle-of-attack behavior.

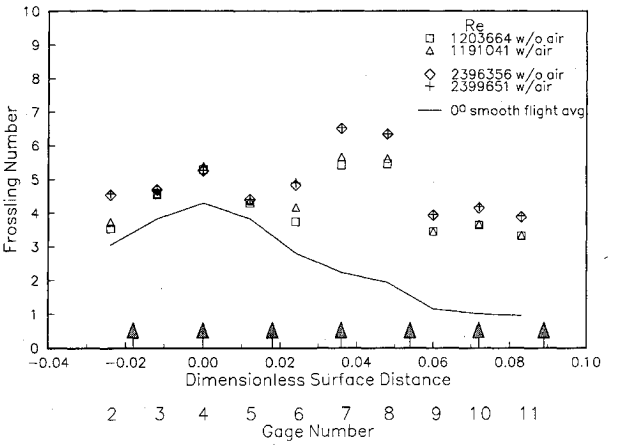

Fig. 4 Frossling number vs dimensionless surface distance: dense 2 roughness, 0-deg angle of attack, $Re=1.2\times10^6$ and 2.4×10^6, IRT data.

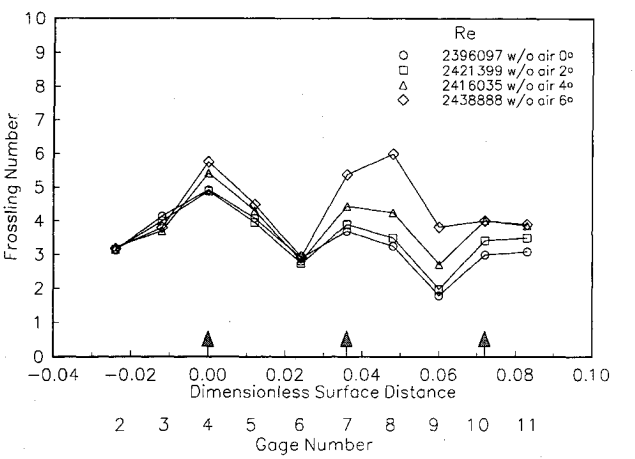

Fig. 5 Frossling number vs dimensionless surface distance: sparse roughness, 0-, 2-, 4-, and 6-deg angles of attack, $Re=2.4\times10^6$, with spray air, IRT data.

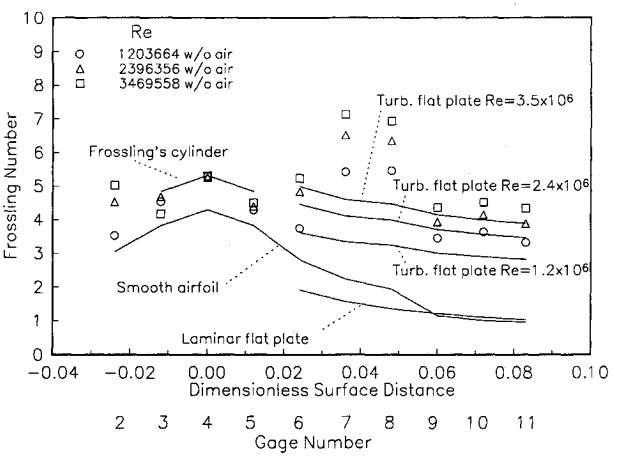

Fig. 6 Frossling number vs dimensionless surface distance: dense 2 roughness, 0-deg angle of attack, IRT data (without spray) vs dimensionless correlations for cylinder[5] and flat plate.[6]

Data were also acquired at a −4-deg angle of attack, which allowed more complete measurement of pressure side heat transfer values. Comparing the −4-deg (pressure side) data with the +4-deg (suction side) data showed that for the roughened airfoil the pressure side experienced lower heat transfer than the suction side.

In computer codes, heat transfer from airfoils is often estimated by using cylinder-in-crossflow heat transfer values in the leading edge region and flat plate heat transfer values farther aft. Figure 6 shows the IRT data for the dense 2, 0-deg, without spray condition compared with the cylinder and flat plate heat transfer values. The heat transfer in the stagnation region for the dense 2 roughened airfoil agrees fairly well with Frossling's[5] smooth cylinder laminar flow solution. Moving downstream on the airfoil, the heat transfer drastically increases, reaching a maximum level near s/c of 0.035, and then decreases to a level fairly consistent with turbulent flow flat plate heat transfer values.[6] The measured Frossling numbers at specific Reynolds numbers are somewhat higher than their respective flat plate turbulent values. However, the higher measured heat transfer may be due to the increase in surface area caused by the roughness elements (3–7% increase on each gauge for the dense roughness patterns) that was not taken into account in the data analysis. It may be mentioned here that the maximum heat transfer is in the same general region, if slightly aft, of ice horn growth observed during glaze ice accretion.[7]

Conclusions

Local heat transfer measurements from a roughened NACA 0012 airfoil were successfully obtained in flight and in the NASA Lewis icing research tunnel using the method and apparatus described in this work. Major conclusions resulting from this study are as follows.

1) The addition of roughness to the airfoil surface drastically increased the heat transfer downstream of stagnation. The roughness elements disturbed the laminar boundary-layer flow and in some cases caused a transition to turbulent flow.

2) Comparison of the flight and tunnel roughened surface data showed that the general effect of increased turbulence was a slight increase in heat transfer, especially at the higher Reynolds numbers.

3) Generally, the roughened surface airfoil cases showed the suction side heat transfer monotonically increasing with angle of attack.

Acknowledgment

This work was supported under Grant NAG 3-72 by the NASA Lewis Research Center, Cleveland, Ohio.

References

[1]Poinsatte, P. E., Van Fossen, G. J., Newton, J. E., and De Witt, J. E., "Heat Transfer Measurements From a Smooth NACA 0012 Airfoil," *Journal of Aircraft*, Vol. 28, No. 12, 1991, pp. 892–898.

[2]Van Fossen, G. J., Simoneau, R. J., Olsen, W. A., and Shaw, R. J., "Heat Transfer Distributions Around Nominal Ice Accretion Shapes Formed on a Cylinder in the NASA Lewis Icing Research Tunnel," AIAA Paper 84-0017, Jan. 1984; see also NASA TM-83557, Jan. 1984.

[3]Schlichting, H., "Experimental Investigation of the Problem of Surface Roughness," NACA TM-823, April 1937.

[4]Poinsatte, P. E., "Heat Transfer Measurements from a NACA 0012 Airfoil in Flight and in the NASA Lewis Icing Research Tunnel," M.S. Thesis, Dept. of Chemical Engineering, Univ. of Toledo, Toledo, OH, June 1989; see also NASA-CR 4278, March 1990

[5]Frossling, N., "Evaporation, Heat Transfer, and Velocity in Two Dimensional and Rotationally Symmetrical Laminar Boundary Layer Flow," NACA TM-1432, Feb. 1958.

[6]Welty, J. R., Wicks, C. E., and Wilson, R. E., *Fundamentals of Momentum, Heat, and Mass Transfer*, Wiley, New York, 1984, p. 370.

[7]Olsen, W. A., Shaw, R. J., and Newton, J. E., "Ice Shapes and the Resulting Drag Increase for a NACA 0012 Airfoil," NASA TN-83556, Jan. 1984.

Incompressible Steady Aerodynamics Using a Standard Finite Element Code

S. De Rosa* and G. Pezzullo†
Centro Italiano Ricerche Aerospaziali, 81043 Capua, Italy

Nomenclature

A = nodal area
n = normal vector
S_B = surface of the body
S_C = surface of the branch cut
S_E = any external surface including the body
V_∞ = asymptotic freestream velocity
∇^2 = Laplacian operator
ϕ = velocity potential

Subscripts

$()_u$ = values of $()$ at the upper side of the trailing edge
$()_l$ = values of $()$ at the lower side of the trailing edge

I. Introduction

In the last decade, great attention has been devoted to the solution of the wave equation using the finite element technique.[1,2] The use of a finite element structural code for general scalar fields can be approached on the basis of an analogy between structural equations of elasticity and those for the relevant scalar fields. For lifting aerodynamic fields, the same approach may be used, but a new problem due to the circulation must be solved. In this Note, a simple way to solve steady incompressible aerodynamic fields around a body is presented. The work extends the common approach for the scalar fields using the standard structural finite element code to lifting flowfields. One of the greatest advantages of this approach is the possibility of using the standard preprocessing tools developed for structural problems to aerodynamic problems. The described approach can be used for general three-dimensional bodies, or multicomponents airfoils, due to the feasibility of realizing an unstructured mesh, as those required by the finite element technique.

II. Theoretical Formulation

The classical aerodynamic problem is to develop the steady, nonviscous, incompressible aerodynamic field around a body. The governing field equation is

$$\nabla^2\phi = 0 \tag{1}$$

with the boundary conditions (Fig.1) as follows.

The body is a streamline:

$$\frac{\partial\phi}{\partial n} = 0 \quad \text{over } S_B \tag{2}$$

Asymptotic condition:

$$\frac{\partial\phi}{\partial n} = V_\infty \cdot n \quad \text{over } S_E \tag{3}$$

Received July 21, 1990; revision received Nov. 15, 1990; accepted for publication Dec. 10, 1990.

*Researcher, Vibration & Acoustic Branch, Via Maiorise. Member AIAA.

†Researcher, Vibration & Acoustic Branch, Via Maiorise.